Electroencephalography and clinical Neurophysiology, 91 (1994) 295–310

EEG 93218

A test of brain electrical source analysis (BESA): a simulation study

W. Miltner [a], C. Braun [a], R. Johnson, Jr. [b], G.V. Simpson [c] and D.S. Ruchkin [d,*]

[a] *Department of Medical Psychology, University of Tübingen, 7600 Tübingen (FRG),* [b] *Department of Psychology, Queens College, CUNY, Flushing, NY 11367 (USA),* [c] *Departments of Neurology and Neuroscience, Albert Einstein College of Medicine, Bronx, NY 10461 (USA), and* [d] *Department of Physiology, University of Maryland Medical School, Baltimore, MD 21201 (USA)*

(Accepted for publication: 27 April 1994)

Summary The present report summarizes the results of a simulation study on the accuracy of Scherg's implementation of spatio-temporal analysis (BESA) for estimating the parameters (wave shape, location, orientation) of the intracranial sources of event-related brain potentials (ERPs) recorded from the scalp. In view of the subjective factors that might influence a solution, 10 subjects, ranging from those with much experience with ERPs and extensive background in the use of BESA to those with little experience with BESA and/or no knowledge of ERPs, independently analyzed a set of simulated somatosensory ERP data. The simulation contained wave forms from 32 electrode sites generated by a combination of 10 dipole sources. The primary question was how faithfully the different subjects would depict the source wave shapes, locations and orientations. Based on the 9 subjects who were familiar with ERPs, the grand-average cross-correlation coefficient between subjects' estimated and actual source wave shapes was 0.89 (standard deviation (S.D.) = 0.17). The grand-average location error, based upon a head diameter of 17 cm, was 1.4 cm (S.D. = 1.0 cm). The grand-average orientation error was 24.4° (S.D. = 20°).

Key words: Source localization; Event-related potentials; Spatio-temporal analysis; Simulation

Recent research in neurology, neuropsychology and psychophysiology indicates an increasing interest in the localization of neural sources that generate event-related brain potentials (ERPs) recordable at the scalp. Different approaches to the problem of brain electrical source analysis (BESA) have been suggested (Nunez 1981, 1986; Fender 1987; Scherg 1990; Lopes da Silva and Spekreijse 1991; Dale and Sereno 1993; Law et al. 1993; Nunez et al. 1994). All of these approaches are based on the assumption that the scalp activity arising from cortical and subcortical neural structures can be described as a pattern of fields emanating from different electrical dipoles that are the result of either extracellular or intracellular electrical currents of large and structured cortical or subcortical neural cell assemblies (Caspers et al. 1984; Speckmann et al. 1984; Nunez 1990).

Spatio-temporal source analysis has been one approach to localization of brain electrical sources (Achim et al. 1988; Scherg 1990; Turetsky et al. 1990). The purpose of the current study was to evaluate the efficacy of spatio-temporal source analysis, as exemplified by Scherg's implementation (BESA), which is commercially available and has been used in a number of recent ERP investigations (Scherg 1984; Scherg and Von Cramon 1985a,b, 1986a,b, 1989; Curio et al. 1987; Braun et al. 1989; Scherg et al. 1989; Simpson et al. 1990; Ebersole 1991; Franssen et al. 1992; Praamstra and Stegeman 1992; O'Donnell et al. 1993; Ponton et al. 1993; Tarkka and Treede 1993; Toro et al. 1993). The Scherg (1990) approach considered the ERP components as arising from multiple neural sources located in different brain regions, whose activity overlaps in time. It was assumed that the activity of all sources will superimpose *linearly* at each site on the scalp, producing complex wave forms with different shapes at different electrode sites. It was further assumed that the sources can be modeled by combinations of dipoles. Thus, in Scherg's spatio-temporal approach, assuming that noise is negligible, the ERP wave form at the kth electrode ($V_k(t)$) is represented by a linear combination of multiple source wave forms ($s_1(t) \ldots s_n(t)$) weighted by coefficients, c_{ki}, that describe the attenuation factor by which the ith source potential propagates to electrode k:

$$V_k(t) = c_{k1}s_1(t) + c_{k2}s_2(t) + c_{k3}s_3(t) + \ldots c_{kn}\, s_n(t) \quad (1)$$

* Corresponding author. Tel.: 410-706-5272; Fax: 410-706-8341; E-mail: druchkin@umab.umd.edu, druchkin@umab.bitnet.

SSDI 0013-4694(94)00145-B

Each dipole source at any given point in time is specified by 6 parameters: the coordinates that specify its position in 3-dimensional space, the 2 angles that specify its orientation in 3-dimensional space, and the strength of the source. The first 5 parameters are embodied in the weighting coefficients, c_{ki}, while the source strength at time "t" is specified by the $s_i(t)$ term. Also embodied in the weighting coefficients is the known electrical conductivity of the tissue through which the field propagates. Thus, in Scherg's formulation, the weighting coefficients are constrained by the biophysical properties of volume conduction of electrical fields through the brain to the scalp. Given knowledge of the electrode locations, the weighting coefficients (c_{ki}) in effect specify the location of the sources, while the $s_i(t)$ specifies the source strength (dipole moment) at time "t."

In the simplest case of only one dipole source and no noise, given knowledge of the geometry and conductivity of the head, measurements from 6 suitably spaced electrodes at a single point in time are all that is required to exactly specify the location, orientation and strength of that dipole. The problem of specifying the source parameters is more complex when the source configuration must be modeled by multiple dipoles and measurements are made in the presence of noise (e.g., the residual EEG in the averaged ERP wave forms). In theory, in the absence of noise, at least 6 electrodes per dipole source would be required to specify all dipoles, and still more electrodes would be necessary if noise is present. In this more complex case, which is the usual state of affairs, exact, unique solutions for the sources are not possible. The accuracy of the solution, which can only be an approximation, generally will improve as more electrodes are employed.

To make this problem more tractable, Scherg capitalizes on the fact that not all sources are simultaneously fully active (i.e., source strength varies over time) and thus, at any given point in time, one can obtain a favorable (i.e., high) ratio of number of electrodes to number of active sources. Scherg achieves the "favorable ratio" by using the entire wave shape of the ERPs in formulating his solution. In somewhat over-simplified terms, even though the number of electrodes may be relatively small in comparison with 6 times the total number of sources, at any given point in time the effective ratio may be sufficient to provide a reasonable approximation of the active source parameters (see Scherg (1990) for a rigorous development of these ideas).

Scherg's implementation (BESA) employs a least-squares fitting algorithm that, in the general case, does not provide a unique solution. Scherg deals with the non-uniqueness problem by using an interactive iterative procedure whereby the user evaluates each successive approximation. In this approach, the user determines the initial approximation and then, after each approximation is computed, determines which parameters will be adjusted and which are held constant for the next iteration. Finally, the user decides when the approximation is satisfactory. Thus, Scherg's approach puts a considerable burden upon the user. Therefore, the quality of the final result may depend on the user's knowledge and experience, and the accuracy of the approximation may be dependent on the user's subjective criteria.

In a series of papers, Scherg and co-workers (Scherg 1984; Scherg and Von Cramon 1985a,b, 1986a,b; Curio et al. 1987) have published patterns of brain electrical sources of early (waves I–V), mid-latency (10–45 msec) and late (45–200 msec) auditory evoked potentials that were localized with this spatio-temporal approach. Additional sources of auditory evoked potentials were published recently (Scherg et al. 1989), including the intracerebral sources of the N100 wave to standard auditory stimuli, the sustained potential, and the mismatch negativity to deviant auditory stimuli of the human AEP (Scherg et al. 1989). In each of these cases, the neural sources localized with the spatio-temporal model corresponded well to findings from intracranial studies. Hence, these results would suggest that this approach to source analysis has significant power and validity.

In view of the fact that subjective considerations may determine a solution, the present study was designed to investigate the accuracy of Scherg's approach. The chief issues were the faithfulness of estimated versus actual (simulated) source wave shapes, and the magnitudes of location and orientation errors. A realistic simulation of multi-channel, multi-source ERPs was created, and 10 subjects, spanning the range from highly experienced with ERPs and extensive background in the use of BESA to no knowledge of ERPs and/or little experience with BESA, were asked to identify the number and parameters of the neural sources that were used to generate the simulated data set. Note that this study did not test the validity of Scherg's head model, since the simulation used the spherical head approximation employed by BESA, nor the validity of the equivalent dipole as a source model, since the simulation used the dipole model employed by BESA.

Methods

Subjects

Solutions were obtained from 10 subjects. Three subjects had considerable experience with BESA, three had some experience with BESA, and four had relatively little experience with BESA. All but one subject, a physicist with no familiarity with ERPs, were ERP

investigators. All the authors, except CB, served as subjects.

In contrast with all the ERP investigators, the physicist employed a markedly different strategy, because he made no attempt to use the concept of bilateral symmetry for ERP sources. Instead, he simply tried to fit the data with as few dipoles as possible. Because several of the sources in the model were bilaterally symmetric pairs, the physicist's results deviated markedly from those of all other subjects. Thus, while the physicist's results (S1) are presented in tabular form, they were not included when computing across-subject means and standard deviations.

Procedure

The simulated data, 32 channels of averaged somatosensory ERPs, "the model," was generated by one of the authors (CB) using the simulation functions contained in the BESA program (version 1.7). The neural sources, 10 dipoles, were based on previous ERP results from our research using somatosensory stimuli in a P300-oddball paradigm (Braun et al. 1989; Miltner 1989). The model was based upon responses to low-probability stimuli delivered to the left middle finger. The head diameter was 17 cm.

The locations, orientations and wave shapes of each dipole are shown in Fig. 1. Dipoles 1 and 2 simulated responses in primary somatosensory cortex, representing the P100 and an early part of the N150. Dipoles 3 and 4 simulated activation of secondary somatosensory association areas representing late parts of the N150. Dipole 5 simulated a P260 component located in central mid-line cortex. Dipoles 6 and 7 simulated P300 activity in the medial temporal lobes. Dipole 8 simulated early slow wave activity in medio-frontal regions. Dipoles 9 and 10 simulated later slow wave activity in dorso-lateral frontal regions. White noise was added to the simulated scalp average reference wave shapes to produce the simulated set of ERP wave forms. The white noise rms level was equal to one-fifth of the mean signal rms level, averaged across the 33 average reference wave shapes. Fig. 2 illustrates the simulated

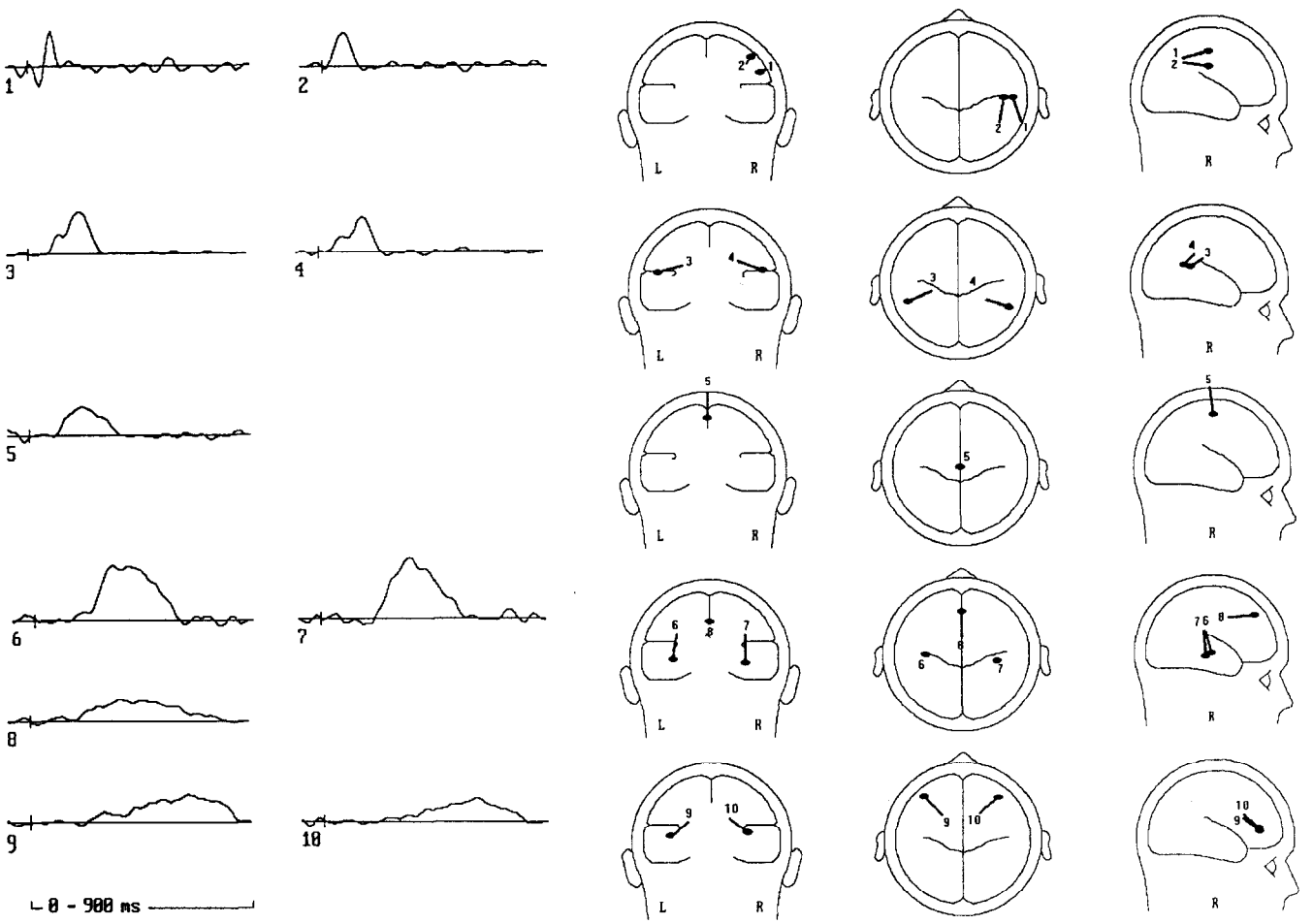

Fig. 1. Locations, orientations and wave shapes of the 10 dipole sources, "the model sources," used to simulate the ERP data. Stimulus onset is denoted by the vertical mark on the time base.

set of ERP wave forms, in average reference format, arrayed to show their approximate locations on the scalp.

Each subject was informed that the data represented somatosensory ERPs recorded over the epoch from 90 msec pre-stimulus to 900 msec post-stimulus (sampling interval = 10 msec) elicited by low-probability stimuli in an oddball paradigm by non-painful electrical stimulation of the left middle finger. Subjects were further informed that "noise" had been added. Most subjects provided a written report covering the strategy and hypothesis used to obtain their solution and noted problems encountered during the procedure.

Data analysis and methods of evaluation

First, each of the dipoles in each subjects' solution was assigned to a corresponding dipole in the model. Since source location and wave shape are inextricably linked in a BESA solution, correspondence between solution and model dipoles was decided on the basis of wave shape similarity[1]. Similarity was assessed by obtaining the maximum of a cross-correlation function computed between the wave forms of a subject's dipole and a model dipole. The cross-correlation function was computed over the latency range of 10–800 msec post stimulus, where the lags extended over ±100 msec. In the case of bilateral homologous pairs, the final assignment was made on the basis of correspondence between subject and model dipole hemispheric location. This procedure was repeated until all subject dipole assignments to a model dipole were made. Across all subjects, there were a total of 5 dipoles that could not be associated with any remaining model dipole and hence were declared spurious.

Amplitudes and latencies of all dipole wave forms were quantified. The wave forms were initially smoothed by a low-pass digital filter with a 25 Hz half-power frequency and a 24 dB/octave slope. Amplitude was measured by computing the average over a latency window centered about each dipole's wave form peak. The latency window width ranged from 30 msec for the shortest latency peaks to 150 msec for the longest latency peaks. Dipole wave form latencies were quantified in 4 ways: (1) peak latency, (2) mid-mean peak latency, (3) onset latency, and (4) offset latency. Mid-mean peak latency, which is sensitive to where in time most of the energy of a wave form is concentrated, was obtained by computing the mean of the latencies where, before and after the peak, the amplitude was 40% of peak amplitude. Onset (offset) latencies were defined as those latencies at which the dipole wave first (last) reached 20% of peak amplitude.

For data presentation purposes, the physicist is designated as S1. All other subjects were ranked according to their average "residual variance" (RV), the smaller the variance, the higher the ranking. BESA provides RV as a measure of the goodness-of-fit of its solution to the actual data at the end of each iteration. An RV function is computed as the ratio of the mean square difference between the solution waves and actual data waves to the mean variance of the actual data waves, averaged across all electrodes at each point in time. BESA further provides an average of the RV over a user specified time interval. The average RV for each subject was calculated over the interval from −90 msec to 900 msec.

Results

Fig. 3 shows the locations and orientations of the model dipoles and each subject's solution and Fig. 4 shows the RV function for each subject. It is evident from these data that no subject obtained an exact solution. Furthermore, there was considerable variation in the number of identified sources, ranging from 6 to 10. In addition, one subject produced a single spurious dipole (S3), one subject produced a spurious bilateral pair of dipoles (S6), and one subject produced two unrelated spurious dipoles (S8). Note that the RV functions tend to have an overall "U" shape, with RV being largest at the start and end of the recording epoch. Since RV is a ratio of error to data signal strength, it is large where the signals are small, even though the error may be small.

Dipole wave shapes and residual variance

The wave shapes obtained by the subjects are superimposed upon the model wave shapes in Fig. 5, with all wave forms scaled to unity rms amplitude. The cross-correlation coefficients between subjects' and model

[1] The combination of anatomical location and temporal dynamics defines a source. A BESA solution is interpreted as an estimate of the locations in the brain of specific temporal patterns of activity. Thus, any measure of the quality of subjects' solutions must take into account this inextricable linkage of anatomical and temporal information. This was our rationale for using wave shape as the measure for assigning correspondences between subjects' solutions and the model. An alternative procedure of assigning correspondences on the basis of least anatomical distance may have produced smaller location errors. However, it would make no sense to say that a subject's error was smaller because there was a model source with a different wave shape nearer to the solution dipole than another, more distant model source with a similar wave shape. Assigning of correspondences between model and subject solution sources on the basis of nearest anatomical location would make sense only for a single time point analysis (i.e., when there is no temporal information). It might be argued that matching model and subject-derived dipoles on the basis of wave shape biases the wave shape correlations towards higher values. However, a high level of correlation cannot be obtained unless the subject's solution produces wave shapes that are similar to those of the model.

dipole wave shapes, and the number of spurious dipoles for each subject are presented in Table I, along with the RV for each subject (averaged over the −90 to 900 msec epoch). The means of the RV and correlation coefficients computed across only the ERP investigators (S2–S10) and, for each investigator, across identified dipoles are also presented in Table I. The grand-mean of the correlation coefficients, over all identified dipoles and ERP investigators, was 0.89 (n = 75, standard deviation (S.D.) = 0.17). Both Fig. 5 and Table I indicate that, in most cases, when subjects identified a dipole, the wave shape was accurately depicted.

The mean RV reflects the contribution of estimation errors that would occur even if there were no noise and errors due to the noise that had been added to the simulated wave forms. Thus, due to the noise, the minimum attainable RV had to be greater than zero. An upper bound for the minimum attainable RV was estimated to be 0.86 by fitting the noisy simulated data with the original (noise-free) set of dipoles. Due to the presence of noise, the locations of the original model dipoles were not at a minimum of the error function. Using the original dipoles as the starting point, further iterations were run to find a minimum error solution for the noisy simulated data. The iterations converged to a solution with an RV of 0.83. The displacements of the noisy minimum-error solution dipoles from the original model dipoles ranged from 0.1 to 1.1 cm (average = 0.48 cm). Thus, an estimate of the theoretically best performance that could be expected of the subjects would be an RV ≈ 0.83 and an average location error ≈ 0.5 cm.

Location and orientation errors

The superposition of locations of the subjects' and model dipoles provides an indication of the accuracy and degree of variability in the subjects' solutions (Fig. 6a and b). The location errors for all subjects are presented in Table II, along with means computed across the ERP investigators (S2–S10), and across identified dipoles for each investigator. The grand-mean location error across all identified dipoles and ERP investigators was 1.4 cm (n = 75, S.D. = 1.0 cm), based on a head diameter of 17 cm.

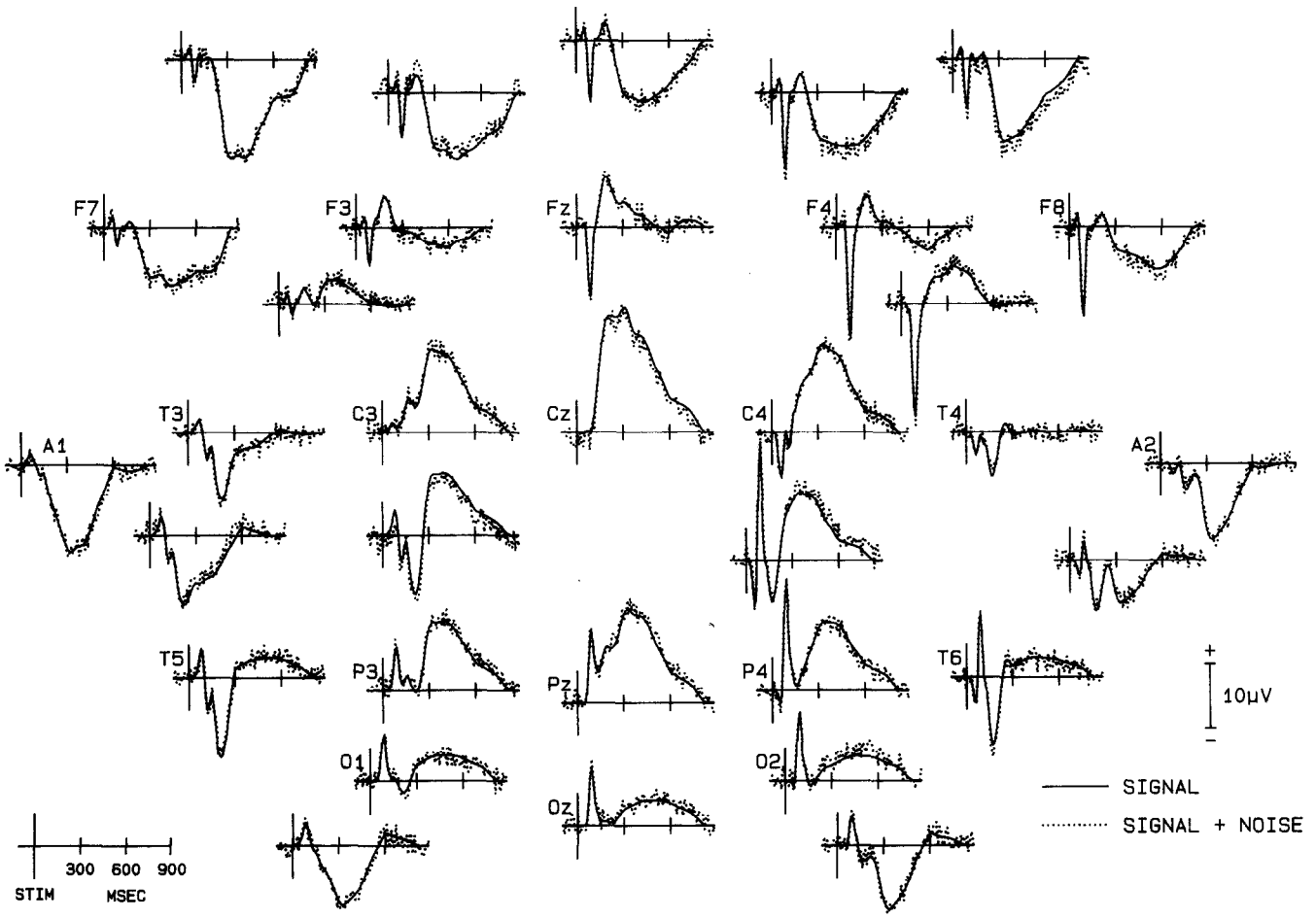

Fig. 2. The simulated scalp ERPs in average reference format. The solid lines indicate the noise-free wave forms generated by the dipole sources indicated in Fig. 1. The dotted lines indicate the signal + noise wave forms that were analyzed by the subjects.

All ERP investigators identified dipoles 2, 3, 4 and 6. All but one ERP investigator (S3) identified dipole 7 and all but one (S2) identified dipoles 9 and 10. S3's error was due to having approximated the dipole 6 and 7 bilateral pair by a single dipole placed approximately midway between these two model dipoles. Although this was a gross resolution and location error, the wave shape of dipole 6 (and, by implication, dipole 7) was accurately depicted (correlation coefficient = 0.99). S2's error derived from his fitting the data only over the range of 40–670 msec. He identified 6 of the 8 dipoles that were largely contained in this range and failed to identify the two long latency dipoles. S2's comparatively low correlation coefficients were partly due to energy from the unidentified long-latency dipoles being spuriously picked-up by the identified shorter latency dipoles. The other ERP investigators identified from 8 to 10 dipoles.

Identification of dipoles 1, 5 and 8 was problematic. When dipole 1 was identified, the subject extracted either only the positive or the negative peak, but not both, which resulted in very low to low correlation coefficients (0.05–0.67). The prolonged activity in the subjects' approximation to dipole 5 (Fig. 5) suggests that the model dipoles 5 and 8 were treated as a composite, and this composite depicted the combined activity of the two dipoles. For the remaining identified dipoles, the subjects' depictions of wave shape were more accurate, with all but one correlation coefficient (S10, dipole 10) greater than 0.73.

Note that, with the exception of the problematic dipoles 5 and 8, the mean across subject (S2–S10) location error for individual dipoles was in the range of 0.58–1.46 cm. Furthermore, although S2 only identified 6 dipoles, his location accuracy was comparable to that of the other subjects (mean error = 1.5 cm, range: 0.3–2.0 cm).

The extent and variability of the subjects' orientation errors, relative to the model dipole orientations, are displayed in Fig. 7. The orientation errors for all subjects are presented in Table III, along with means computed across the ERP investigators (S2–S10), and across identified dipoles for each investigator. The grand-mean orientation error, across all identified

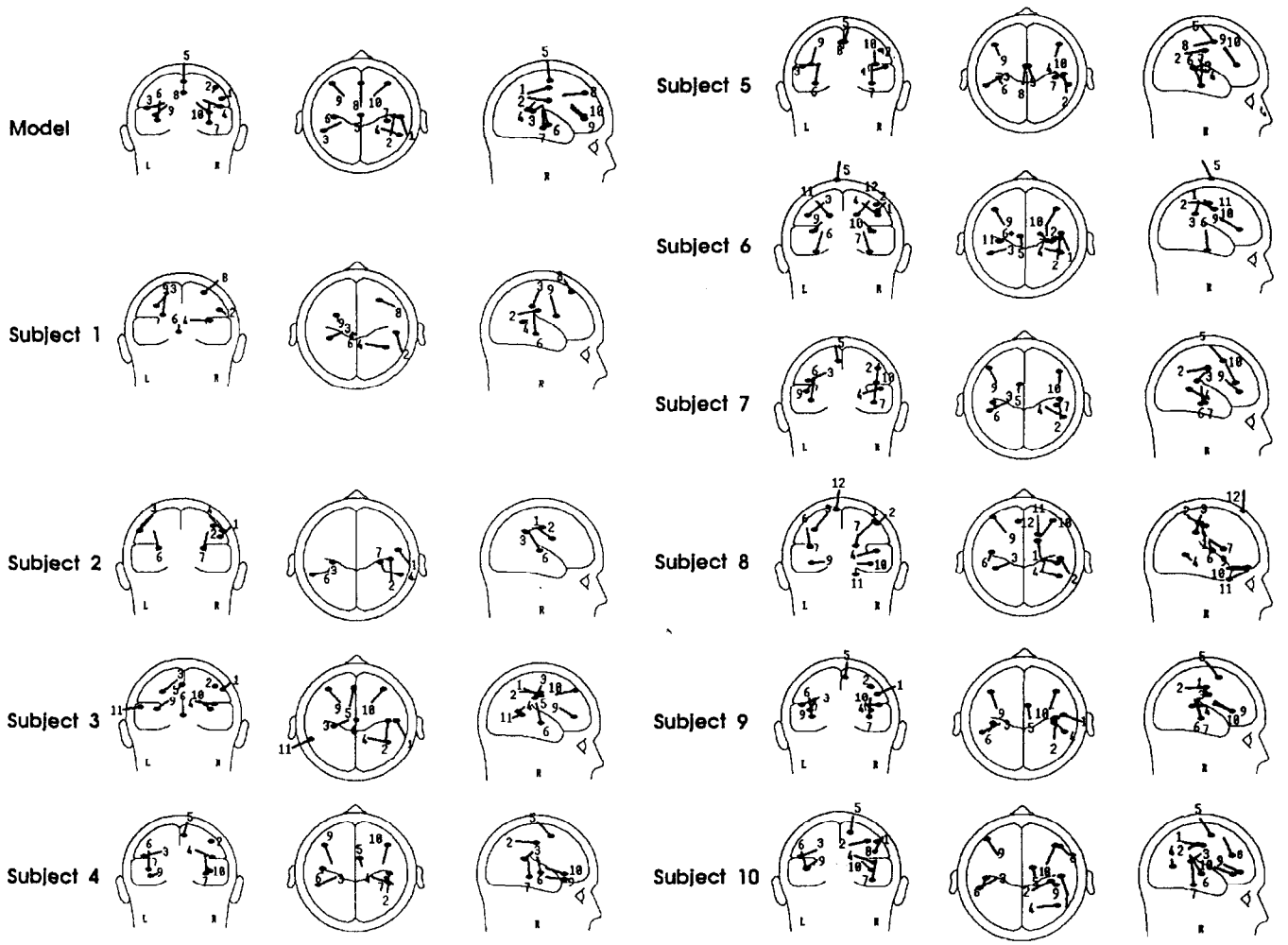

Fig. 3. Locations and orientations of the dipoles for the model and each subject's solution.

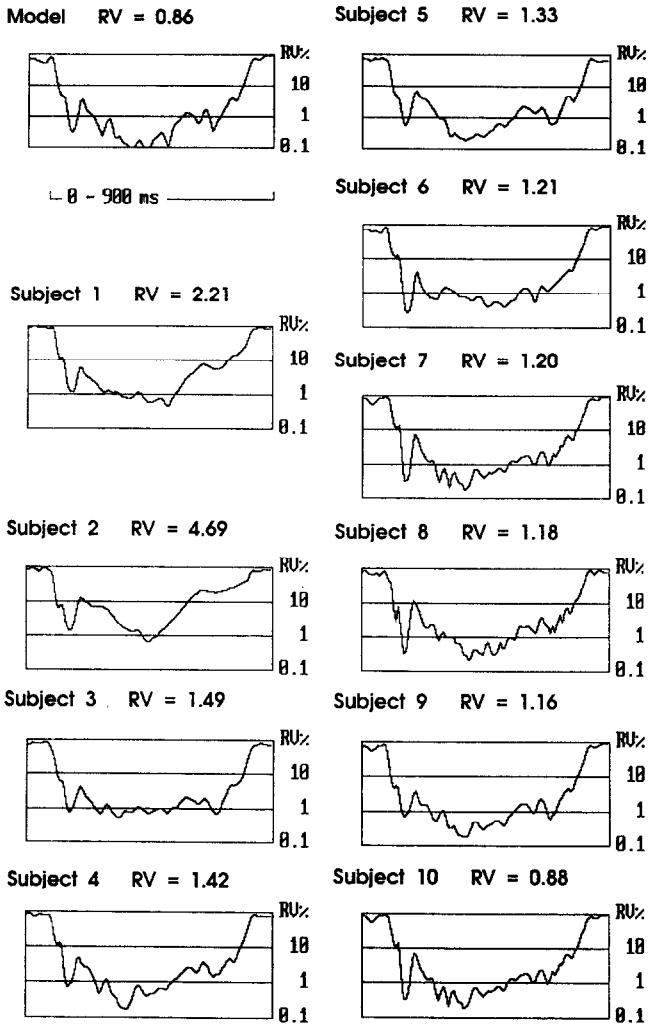

Fig. 4. Percent residual variance for the model and each subject's solution, plotted as a function of time. The number above each graph indicates the average residual variance over the −90 to 900 msec analysis epoch.

TABLE I

Cross-correlation coefficients between subject and model wave forms.

Subj	RV	Dipole										Mean	No. of spurious dipoles
		1	2	3	4	5	6	7	8	9	10		
1	2.21		0.65	0.95	0.85		0.88		0.96	0.96		0.88	0
2	4.69	0.05	0.76	0.97	0.98		0.93	0.97				0.78	0
3	1.49	0.27	0.93	0.95	0.94	0.73	0.99			1.00	0.89	0.84	1
4	1.42		0.93	0.99	0.92	0.85	0.99	0.99		0.99	0.99	0.96	0
5	1.33		0.87	0.99	0.96	0.92	0.99	0.93	0.74	0.99	0.97	0.93	0
6	1.21	0.56	0.94	0.99	0.94	0.95	0.97	0.98		0.99	0.94	0.92	2
7	1.20		0.81	0.99	0.96	0.80	0.99	0.91		0.99	0.97	0.93	0
8	1.18	0.66	0.87	0.99	0.95		0.96	0.96		0.86	0.82	0.89	2
9	1.16	0.20	0.88	0.98	0.95	0.91	0.99	0.95		1.00	0.96	0.87	0
10	0.88	0.67	0.77	0.91	0.93	0.90	1.00	0.97	0.86	0.96	0.64	0.86	0
Mean	1.62	0.40	0.86	0.97	0.95	0.87	0.98	0.96	0.80	0.97	0.90		
S.D.		0.26	0.07	0.03	0.02	0.08	0.02	0.03	0.08	0.05	0.12		

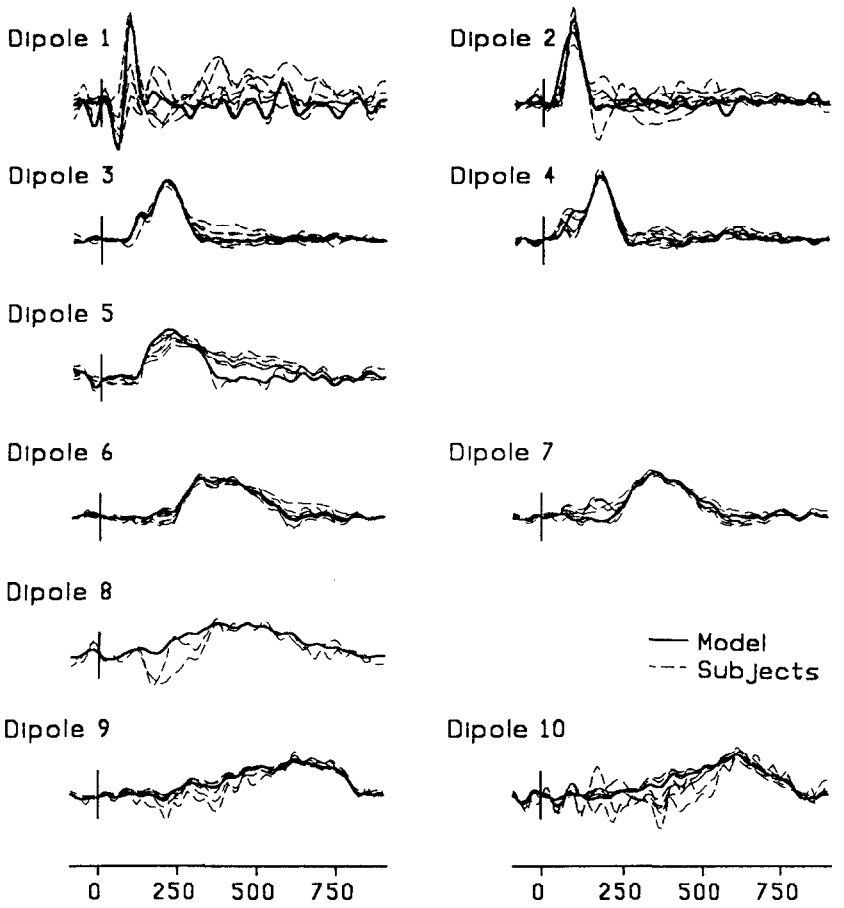

Fig. 5. For each dipole, superimposed model wave shape (solid lines) and wave shapes from each subject's solution (dashed lines). All wave forms have been scaled to the same rms level.

dipoles and ERP investigators, was 24.4° (n = 75, S.D. = 20°). With the exception of the problematic dipoles 1, 5 and 8, the mean across subject (S2–S10) orientation error for individual dipoles was in the range of 13.4–28°.

Dipole wave form latencies and amplitudes

The latencies and amplitudes of the subjects' dipole solutions, averaged across ERP investigators, are presented in Table IV. To facilitate comparisons between the model and subject results, for each parameter

TABLE II

Location errors in centimeters for 17 cm diameter head.

Subj	Dipole										Mean
	1	2	3	4	5	6	7	8	9	10	
1	2.01	2.46	1.51			3.59		3.70	3.40		2.78
2	1.49	0.33	2.03	1.96		1.51	1.80				1.52
3	0.92	0.43	3.16	1.10	4.95	3.84			0.31	0.30	1.87
4		0.28	0.44	1.20	1.89	0.91	0.52		1.71	1.58	1.07
5		1.05	0.58	1.15	1.20	1.15	0.62	3.76	1.30	1.18	1.33
6	1.40	0.19	1.68	1.72	2.88	1.68	1.34		0.74	0.70	1.37
7		0.73	1.02	0.77	2.17	0.61	0.86		0.84	1.65	1.08
8	2.44	0.50	2.62	1.18		1.88	4.04		1.71	2.11	2.06
9	0.65	0.52	0.19	0.95	1.70	0.64	0.48		1.01	1.11	0.81
10	1.27	1.20	0.49	1.62	1.76	0.89	1.14	5.17	0.64	1.18	1.53
Mean	1.36	0.58	1.36	1.29	2.36	1.46	1.35	4.46	1.03	1.23	

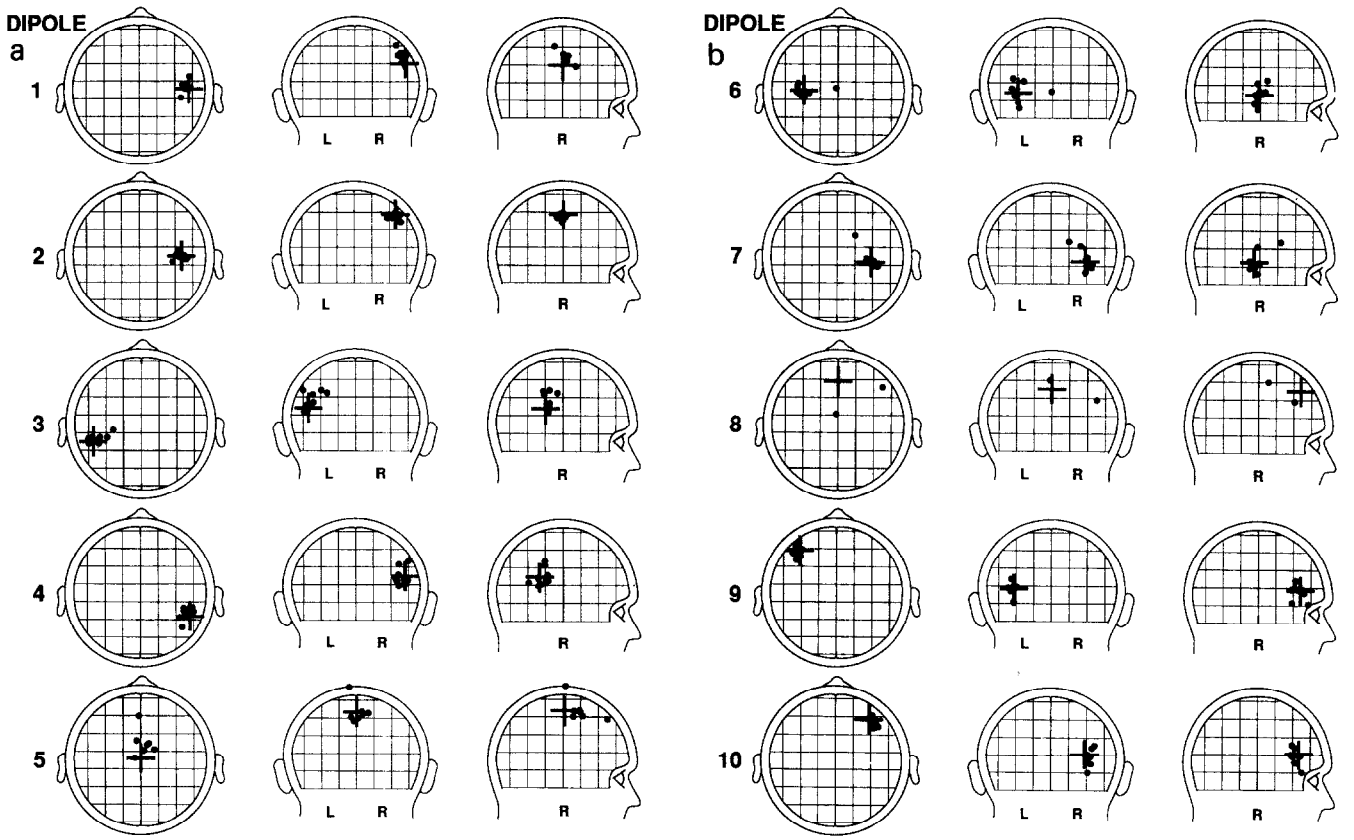

Fig. 6. Left: locations of subjects' solution dipoles (dots) and the model dipole (center of cross) for dipoles 1–5. Based upon a head diameter of 17 cm, the distance between grid lines is 2 cm and the distance from the center of the cross to the end of each arm 1.5 cm in this part and the right-hand part. Right: locations of subjects' solution dipoles (dots) and the model dipole (center of cross) for dipoles 6–10.

there are 3 rows in Table IV: (1) the model values, (2) the across subjects mean values, and (3) the across-subjects mean absolute errors. Dipole 1^- refers to the initial negative peak of dipole 1 while dipole 1^+ refers to the subsequent positive peak. The peak and mid-mean latencies are indicators of when the dipole was maximally active, while onset and offset latencies indicate the temporal extent of the dipoles' activity. In practice, these measures may be used to address the issue of whether the timing of various dipole processes is serial, parallel or cascade.

The peak latencies were most accurately estimated. With the exception of dipole 8 (identified only by S4 and S10), the mean absolute error was less than 19 msec. S10's estimate of dipole 8 peak latency corresponded to the actual model peak latency (370 msec),

TABLE III

Orientation errors in degrees.

Subj	Dipole										Mean
	1	2	3	4	5	6	7	8	9	10	
1		26.3	32.5	20.1		13.0		74.1	44.1		35.0
2	26.1	12.8	36.0	28.0		25.6	32.4				26.8
3	16.8	17.2	26.1	13.3	93.0	6.7			4.8	9.6	23.4
4		20.0	0.9	3.4	35.5	6.6	1.9		31.9	34.1	16.8
5		18.6	9.1	41.6	33.4	4.1	4.0	8.8	29.4	31.1	20.0
6	16.9	18.3	25.2	17.0	18.1	14.8	15.8		12.3	17.5	17.3
7		13.9	7.6	34.4	34.6	1.2	9.9		14.7	47.5	20.5
8	119.8	54.9	35.9	33.3		19.4	55.0		26.9	32.3	47.2
9	52.7	13.7	8.6	31.6	31.8	15.8	10.2		21.8	27.3	23.7
10	1.0	49.8	9.6	20.2	25.2	26.2	12.6	71.7	11.8	24.7	25.3
Mean	38.9	24.4	17.7	24.8	38.8	13.4	17.7	40.3	19.2	28.0	

but S4's estimate was 90 msec too long. The estimates of the mid-mean latencies, which depended upon the precision of the estimates of amplitudes on the rising and falling slopes of the dipole wave shapes, were less accurate than the estimates of the peak latencies. The errors were greatest for dipole 5, whose estimated wave shape usually consisted of a composite of the actual dipole 5 wave form and a longer latency fragment from the actual dipole 8, and for dipoles 8 and 10, which had long duration, slowly varying wave shapes.

The estimates of the onset and offset latencies were most prone to error, since they depended upon the precision of amplitude estimates from the initial and final low-amplitude sections of the rising and falling slopes of the dipole wave shapes. The errors were greatest for slowly changing slopes in epochs of heavy overlap (onsets of dipoles 8, 9 and 10, offset of dipole 8) and for the offset of the dipole 5 (whose estimated wave shape usually was a composite of dipoles 5 and the later dipole 8). Although the onset latency errors were relatively large in comparison with the actual onset latencies, it is important to note that the *sequence* of dipole onsets was estimated with reasonable accuracy. Spearman rank-order correlation coefficients were computed between model and identified dipole onset latencies for each subject. The across-subjects mean of the correlations was 0.944 (range: 0.812–0.992).

Relative accuracy tended to be less for amplitudes than for latencies. The ratio of mean absolute error to model amplitude ranged from 0.15 to 1.06, which is an order of magnitude greater than the ratios for peak and mid-mean latencies.

Residual variance measure

The utility of the RV measure was explored by computing a series of Spearman rank order correlation coefficients between RV and other performance measures, with ERP investigators as the independent variable. These analyses revealed that RV was clearly related to the number of model dipoles identified ($Rs = -0.692$, $P < 0.05$), but was not related to average location error across identified dipoles ($Rs = 0.07$),

TABLE IV

Latency and amplitude measures from dipole wave forms.

	Dipole										
	1^-	1^+	2	3	4	5	6	7	8	9	10
Peak latencies											
Model	50	90	80	210	170	210	320	350	370	620	610
Mean	48	92	90	206	173	226	330	346	415	624	610
Mean abs. err.	2.0	1.7	10.0	6.7	3.3	18.6	14.4	3.8	45.0	8.8	10.0
Mid-mean latencies											
Model	45	95	85	190	155	230	395	375	430	590	575
Mean	44	92	92	201	168	288	404	371	475	603	598
Mean abs. err.	5.0	3.3	6.7	11.1	17.8	57.9	15.6	9.4	45.0	15.0	46.3
Onset latencies											
Model	20	70	30	100	60	120	240	240	210	260	320
Mean	18	68	51	102	87	123	238	224	320	343	406
Mean abs. err.	2.0	12.5	21.1	2.2	35.6	2.9	11.1	28.8	110.0	82.5	93.8
Offset latencies											
Model	60	120	130	280	230	340	570	540	760	800	790
Mean	70	115	140	312	240	546	586	519	640	809	788
Mean abs. err.	14.0	10.0	10.0	32.2	10.0	205.7	31.1	28.8	120.0	8.8	2.5
Amplitudes (arbitrary units)											
Model	−1.1	2.6	3.4	4.1	3.1	3.0	6.4	6.5	2.4	2.4	2.3
Mean	−1.0	2.0	5.6	5.2	3.9	3.0	6.7	6.5	1.9	2.1	2.0
Mean abs. err.	0.5	2.8	2.3	1.3	1.0	1.2	2.1	2.1	0.6	0.4	0.3

Entries in the "Model" rows were obtained from the model wave forms. Entries in the "Mean" rows are averages of values obtained from the ERP investigators' wave forms. Entries in the "Mean abs. err." rows are averages of the absolute value of the difference between the corresponding measures obtained from the ERP investigators' and model wave forms. All latencies are in milliseconds.

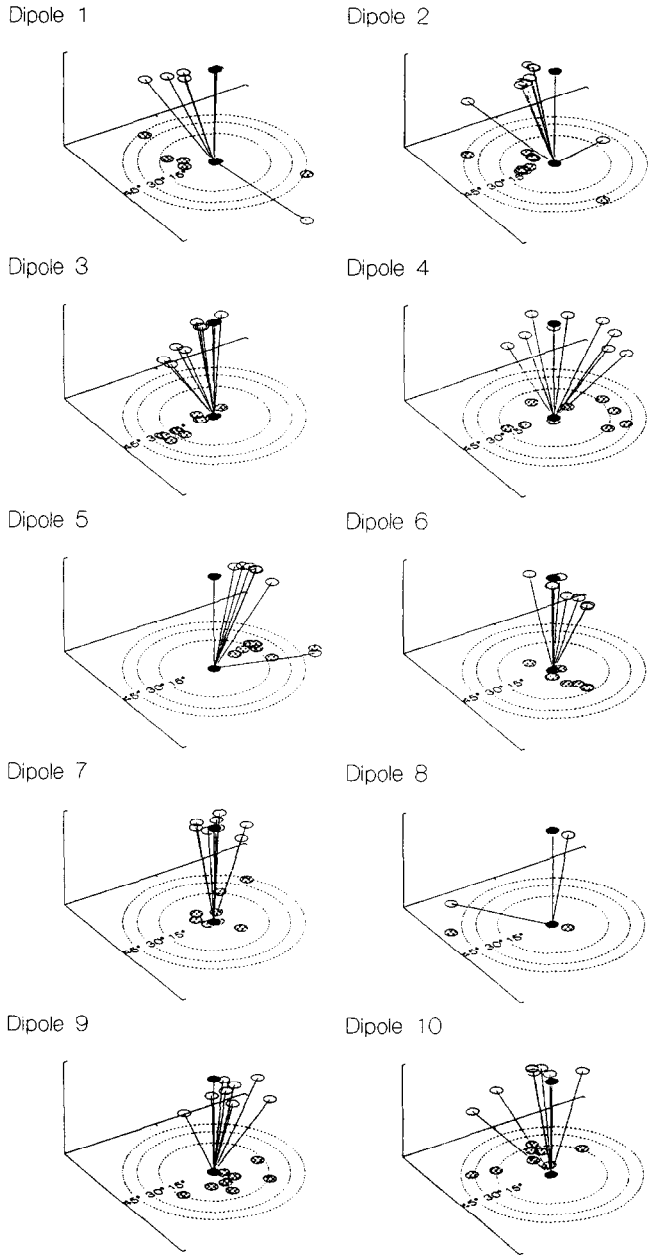

Fig. 7. Relative orientations of each subjects' solution dipoles and the model dipole. The vertical line with a solid disk in the center of the concentric circles represents the model dipole (rotated to be perpendicular to the horizontal plane) while the lines with open disks represent the solution dipoles' orientations, relative to the model dipole. The hatched circles represent the projections of the dipoles onto the horizontal plane, indicating the degrees of deviation from the model.

average orientation error ($Rs = -0.27$), or average correlation coefficient ($Rs = -0.10$).

Discussion

The results of this simulation study provide an indication of the accuracy and replicability of the BESA approach to characterizing the neural generators of ERPs. To represent the likely complexity of a typical ERP data set with short- and long-latency components, this simulation employed ERP wave forms based upon 10 sources with varying degrees of temporal overlap and a variety of temporal wave shapes, spatial locations and orientations. To examine the replicability and generalizability of obtaining similar solutions, we tested a range of subjects, in terms of their previous ERP experience and previous experience in the use of BESA. Subjects with ERP experience located sources with an accuracy of about 1.4 cm, with a high degree of source wave shape correspondence ($\rho = 0.89$) and peak latency errors that were usually between 2 and 19 msec. No one, however, was able to obtain exactly the entire configuration (locations and orientations) of the 10 original dipoles.

Strategy

Whether a source was identified, and the extent of the location error, depended upon its spatial proximity to, similarity of orientation and amount of temporal overlap with other sources. However, users' strategies and expectations also clearly influenced the number of sources obtained and the accuracy with which they were obtained.

The most glaring example of how a user's strategy can affect a solution is the contrast between S1 (the physicist) and the ERP investigator subjects. The physicist was selected because he had considerable analytical expertise but a complete lack of knowledge concerning the neurophysiological basis of ERPs. His lack of familiarity with ERPs was reflected in his overall strategy, which was to obtain a best mean square fit with the least number of sources, without exploring the possibility of bilaterally homologous dipoles. Thus, he fitted a number of bilateral pairs with single sources and accepted a solution with only 6 (poorly located) dipoles.

S2 also settled for only 6 sources. However, this was due to his decision to fit only the data up to 670 msec, and thus he missed the longest latency sources (dipoles 8, 9 and 10). Nevertheless, the sources he did identify were located with an average error of 1.5 cm. S3 used a single mid-line dipole to account for the activity of the dipoles 6 and 7 (a bilateral pair). This error occurred because S3 used the Music-Image feature of BESA to make an initial estimate of the source dipoles. This procedure is best at resolving sources with uncorrelated activity (see the BESA manual) and, hence, has a tendency to represent bilateral pairs of dipoles that have similar wave forms by a single dipole.

The most successful strategy, in terms of minimizing average location error, was employed by S9. S9 used a 15 Hz low-pass digital filter to first smooth the data wave forms (the BESA default filter for data with a 10

msec sampling interval was 25 Hz). In order to minimize source interactions, BESA's Minimum Energy Criterion (EC ~0.20) was always active. The data were initially fitted with two laterally homologous regional sources. The locations of the regional sources, constrained to be laterally symmetric, were first allowed to vary. Then the orientations of the constituent dipoles were varied, after which the dipoles were released while retaining the lateral symmetry constraint for two pairs (which ultimately converged to source dipoles 3 and 4, and source dipoles 6 and 7). The other two dipoles became the basis for source dipoles 2 and 5. Additional dipoles were added, one at a time. After some experimentation, the dipoles that evolved into source dipoles 9 and 10 were constrained to have laterally homologous locations. Orientations of laterally homologous dipole pairs were not constrained. Location constraints were only released when the solution was nearly complete. S9's strategy was heavily influenced by his knowledge of ERPs. Thus, to obtain plausible source wave shapes, he employed BESA's Variance Criterion, which maximizes temporal activity within a specified epoch and minimizes it outside of that epoch. Source dipoles 2, 3, 4, 6 and 7 were expected initially. S9 also expected a "source dipole 1," but not with an orientation that was so similar to that of source dipole 2 and not with the actual degree of temporal overlap with source dipole 2.

Spurious dipoles

Three subjects obtained spurious dipoles. In S3's solution, the model dipole 3 was "bracketed" by his estimate of dipole 3 and an additional dipole 11. This spurious dipole accounted for early, low-intensity activity of model dipole 3, while most of the remaining activity was accounted for by his dipole 3. S6 had an analogous error in his solution for the dipole 6 and 7 bilateral pair. He bracketed this model bilateral pair with two bilateral pairs with similar wave shapes, one above and one below the model dipoles. The higher pair was most different from the model and hence designated spurious (dipoles 11 and 12). S8 produced 3 dipoles with wave shapes that corresponded to the model bilateral pair of dipoles 6 and 7. The location of S8's left hemisphere dipole was in reasonable correspondence with dipole 6, while S8's right hemisphere dipoles bracketed dipole 7, with a dorsal-anterior dipole being more distant and hence designated spurious (dipole 11). In order to test the completeness of his solution, S8 introduced a dipole 12. This dipole indicated that a small, but not negligible, amount of signal energy had not been accounted for by dipoles 1–11. However, S8 was unable to obtain a plausible location for this dipole and hence left it on the surface of the head.

Errors of omission

Errors of omission were generally the result of poor resolution, with the energy of the omitted dipole combined with that of another source. For example, most subjects failed to obtain two different dipoles for model dipoles 5 and 8, even though they were about 5 cm apart. Rather, they obtained a single dipole which, in the time domain, was a composite of dipoles 5 and 8 and was located between dipoles 5 and 8. Since the wave shape of this composite dipole was more similar to dipole 5 than to 8, it was defined as dipole 5. The 3 subjects who did identify dipole 8 did so with gross location errors (4–5 cm). This resulted in dipoles 5 and 8 having the second largest and largest location errors.

Six of the 9 ERP investigators were able to differentiate dipoles 1 and 2 to some degree. However, due to the high degree of temporal overlap and similarity in orientation, this differentiation was not complete in the time domain. The overlap was such that the voltage field and current source density maps in the time interval of the positive peaks of these two dipoles displayed one relatively sharp focus. In those cases where dipole 1 was not found, dipole 2 was able to assume the composite temporal activity pattern of both sources 1 and 2 with little location error.

Missing dipoles did not appear to affect markedly the goodness of the solutions for the correctly identified dipoles. For example, in the present study, missing dipoles 1 and 8 did not prevent the solution from including all other active brain regions and their temporal activation patterns.

Residual variance measure

The overall residual variance (−90 to 900 msec) was only correlated with the number of dipoles identified. It had negligible correlation with a subject's average location error, average orientation error or average wave form correlation coeficient. One reason for these low correlations was that when fewer dipoles were identified, the tendency was to identify only the easier to resolve dipoles. Thus, for subjects who identified more dipoles, the across dipole averages of the correlation coefficients, location errors and orientation errors tended to be diluted with smaller correlation coefficients and larger errors. This was especially apparent for S10, who identified all 10 dipoles and had the smallest RV, but whose across dipole average errors were markedly increased due to his estimate of dipole 8, a dipole which was not found by most other subjects.

While the low correlation of RV with the dipole location and orientation parameters may be partly due to the confounding factor of number of dipoles identified, studies by Cuffin et al. (1991) and Snyder (1991) suggest that there may be an inherent insensitivity of RV to location errors. Snyder (1991) conducted a simulation study which indicated that RV was relatively

unresponsive to perturbations of dipole parameters. In a study of localization errors for dipoles produced by passing current through intracranial electrodes, Cuffin et al. (1991) found that location error could be large even when there was a close correspondence between actual surface potentials and surface potentials computed from the estimated location of a dipole. Thus, these various findings suggest that, while RV may be a useful measure of the completeness of a solution, it may not be able to tell the user whether the identified dipoles are accurately located.

Limitations of the simulation

The simulation used in the present study has limitations which restrict the scope of this evaluation of BESA. These limitations fall into 3 categories: (1) simulation of the head model, (2) simulation of the individual sources, and (3) simulation of the noise. The same head model (single shell Ary-corrected approximation of a 3-shell concentric spheres head model) was used both to generate the simulated data set and by BESA to obtain the solution. Thus, there could be no evaluation of errors introduced by BESA's use of the Ary approximation as a model for an actual head[2]. The accuracy of the inverse solution has been shown to increase when more realistic approximations are used as models for an actual head (Meijs and Peters 1987; Hämäläinen and Sarvas 1989; Meijs et al. 1989). Thus, had the data been simulated with a more realistic head model, then the errors would have been larger, but probably not by too great an amount (Cuffin 1985, 1990, 1993; Cuffin et al. 1991). Cuffin et al. (1991) found that location errors for a dipole created by stimulation of intracranial electrodes were relatively insensitive to spherical model parameters. Cuffin's analytical studies (Cuffin 1985, 1990, 1993) indicated that discrepancies between actual and model head shape, geometry of skull and scalp thickness, and location of fissures generally produced localization errors of less than 1.0 cm, although this depended to some degree on the type of model and the depth of the sources, being somewhat larger for deeper sources (e.g., Peters and Wieringa 1993). A recent simulation study of localization errors due to use of a 3-shell spherical model found errors of the order of 2 cm (Roth et al. 1993). However, the Roth et al. simulation posited only 21 electrodes with little coverage of inferior scalp, and the largest component of the errors was along the z-axis (vertical dimension).

[2] The Ary approximation produces larger location errors than true 3-shell and 4-shell head models (Zhang and Jewett 1993; Berg and Scherg 1994). The most recent version of BESA (Version 2.0) employs a more accurate 4-shell approximation (Berg and Scherg 1994).

The second limitation of the present simulation was due to the fact that the single point sources used to generate the present data set were artificial. Actual brain sources have more extended and complex geometries. Since BESA uses point dipoles to approximate brain generators, errors introduced by this approximation were not evaluated by this simulation.

The third limitation was due to the simulated noise not being completely realistic. Since the on-going EEG does not have a flat power spectrum, the white noise used here was probably more readily filtered from the signal wave forms than may usually occur with real data. Also, this simulation did not examine a range of signal-to-noise ratios (only a 5:1 ratio was used). Signal-to-noise ratio may well affect accuracy of a BESA solution.

Finally, the results apply only to a 32-electrode montage. Greater or lesser accuracy may have been achieved had more (e.g., 64) or fewer (e.g., 16) electrodes been used.

Other studies

The accuracy with which source dipoles can be located using scalp recordings has been examined previously in a number of studies (see Cohen and Cuffin 1991 for a review). Cohen et al. (1990) and Cuffin et al. (1991) passed current between depth electrodes that had been implanted in epilepsy patients for monitoring purposes and then used concurrently obtained scalp EEG recordings to estimate the location of the dipole formed by the electrode pair. The average location and orientation errors were approximately 1.1 cm and 14°. Achim et al. (1991) conducted a simulation study directed primarily at the effects of physiological noise on spatio-temporal modeling of 3 dipoles in a homogeneous sphere. The range of localization errors for "correct" solutions (which left no consistent signal in the residual) would have been equivalent to 0.43–2.21 cm in the current simulation. Mosher et al. (1993) developed general formulas for computing the lower bound on the localization error for one or two dipoles in a 4-spherical shell head model. They computed the lower bounds for a number of specific one and two dipole cases in which a single time point was used. The cases considered in the Mosher et al. study were not identical with the current simulation, so that a precise generalization from their results to the current study cannot be made. However, a rough extrapolation from their findings suggests that the location errors for the current simulation might be in the 1–3 cm range. Mosher et al.'s (1993) results further indicated that localization error is dependent upon the distance between the source dipole and the recording electrodes, with a substantial increase in error as the electrode-source distance increases. This suggests that if sources are expected to be widely distributed in the brain, then

a good strategy would be to place electrodes widely over the scalp, for as broad coverage as possible.

The above studies used fewer sources and different assumptions and approaches to the issue of source localization errors. Moreover, they did not address the effect of user interaction with the localization process. Nevertheless, taken together the location errors in these prior studies were of the same order of magnitude as in the current study.

Conclusion

This study indicates that the BESA implementation of spatio-temporal analysis may not provide an exact solution. Its accuracy will depend upon the number of sources involved and their relative locations, orientations and temporal overlap in the real data. Since this cannot be known by the experimenter, the BESA solution must be interpreted with caution. Its localization errors may range from extremely small to being on the order of 2–3 cm, and it may miss some sources that exist in the real data. Consequently, BESA should not be considered the final answer. Although valuable, it should not be the sole means for inferring the characteristics of ERP generators. Information from other approaches, such as topographic profile analysis, voltage field and current source density maps, also should be employed. When combined with other types of analyses, spatio-temporal analysis can provide important perspectives that enhance understanding of the data.

The results of this study do indicate that analyses of ERP scalp data with spatio-temporal analysis can yield valuable information. It provides a decomposition of the complex overlapping componentry of fields on the scalp into the more informative underlying componentry in the brain. The obtained wave forms do appear to accurately depict temporal dynamics of the underlying components. It also provides a depiction of electrophysiologically active brain regions. While there were location errors, they did not appear to be such as to render the depiction useless. Thus, the findings suggest that BESA (and similar spatiotemporal dipole analysis methods) can provide reasonable estimates of the spatial and temporal characteristics of the brain generator activity underlying ERPs. Overall this represents an advancement relative to the capabilities for estimating ERP generators from surface topography alone. The results here suggest that BESA may be effectively used in studies that combine ERP data with those obtained from techniques that measure brain metabolism, such as positron emission tomography (PET) and functional magnetic resonance imaging (fMRI). Possible ERP generator locations obtained from PET and fMRI results could be used to constrain BESA so that the ERP dipole sources correspond to metabolically active brain areas. Such melding of the superior spatial resolution of the PET and fMRI techniques with the superior temporal resolution of ERPs should greatly enhance our understanding of brain activity.

Although the current simulation does not provide proof of the validity of spatio-temporal analysis, it has examined to a first approximation some of the issues concerning the accuracy of BESA for estimating the generators of ERPs. There are, however, a number of issues that should be addressed by future simulation studies, such as how effectively BESA deals with spatially extended sources and how well BESA can distinguish between an extended source near the surface of the brain and a deep source[3]. The effects of head model inaccuracies also warrents further investigation. As more simulations are conducted to test different aspects of BESA, as more researchers apply BESA to real data, as solutions are replicated across laboratories, and as convergence with other measures is examined, we will be better able to evaluate the utility and validity of BESA and other spatio-temporal analysis procedures.

We thank Dr. Michael Scherg for providing a copy of his program for generating the simulated data and analyzing results and for an excellent tutorial introduction to his method. We also thank Drs. Patrick Berg, Reza Momenan, Brian O'Donnell, Terry Picton, Michael Scherg and Arno Steitz for their collaboration in this study and the large amount of time they spent in estimating the sources of the simulation. We further thank David Mahaffey for his assistance in preparing the figures.

This research was supported by a grant from the Deutsche Forschungsgemeinschaft Bonn (SFB, 307, B2) to WM, by U.S.P.H.S. grants from the National Institute of Neurological Disorders and Stroke (NS 11199) to DSR and (NS 27900) to GVS.

[3] Scherg has formulated 3 elementary simulations of superficial extended, radially oriented sources located 0.2 cm below the surface of the cortex. The single dipole that best fits such distributed sources is also radial, located near the center of, and deeper than, the distributed source. The diameters of the sources were 1.6, 3.2 and 4.6 cm, and the corresponding best fitting single dipoles were located, respectively, 0.21, 0.73 and 1.38 cm below the distributed sources. Attempts to fit the superficial distributed sources by deeper dipoles result in a marked increase in RV. Examination of the voltage fields over the entire upper hemisphere of the head (i.e., including electrodes at inferior locations such as Cb1, Cb2 and the eyes) of the superficial distributed source and a single radial dipole located along a radial line through the center of the distributed source, indicates that the fields are more alike for a single dipole near the superficial source than for a deep dipole. Scherg's simulation does not fully answer the question of whether BESA generally can distinguish between superficial distributed sources and a deep source. However, it does indicate that to make such a distinction the electrode montage should be widely dispersed, including inferior head locations. A more complete test should simulate a numerous variety of sources, and not just a single distributed superficial source which does not require user interaction.

References

Achim, A., Richer, F. and Saint-Hilaire, J.M. Methods for separating temporally overlapping sources of neuroelectric data. Brain Topogr., 1988, 1: 22–28.

Achim, A., Richer, F. and Saint-Hilaire, J.-M. Methodological considerations for the evaluation of spatio-temporal source models. Electroenceph. clin. Neurophysiol., 1991, 79: 227–240.

Berg, P. and Scherg, M. A fast method for forward computation of multiple-shell spherical head models. Electroenceph. clin. Neurophysiol., 1994, 90: 58–64.

Braun, C., Miltner, W. and Scherg, M. A study on the source localization of the late components of the AEP and SEP using a spatial-temporal dipole model. Psychophysiology, 1989, 3: 314.

Caspers, H., Speckmann, E. and Lehmkueller, A. Electrogenesis of slow potentials of the brain. In: T. Elbert, B. Rockstroh, W. Lutzenberger and N. Birbaumer (Eds.), Self-Regulation of the Brain and Behavior. Springer, Berlin, 1984: 26–41.

Cohen, D. and Cuffin, B.N. EEG versus MEG localization accuracy: theory and experiment. Brain Topogr., 1991, 4: 95–103.

Cohen, D., Cuffin, B.N., Yunokuchi, K., Maniewski, R., Purcell, C., Cosgrove, G.R., Ives, J., Kennedy, J.G. and Schomer, D.L. MEG versus EEG localization test using implanted sources in the human brain. Ann. Neurol., 1990, 28: 811–817.

Cuffin, B.N. Effects of fissures in the brain on electroencephalograms and magnetoencephalograms. J. Appl. Phys., 1985, 57: 146–153.

Cuffin, B.N. Effects of head shape on EEGs and MEGs. IEEE Trans. Biomed. Eng., 1990, BME-37: 44–52.

Cuffin, B.N. Effects of local variations in skull and scalp thickness on EEGs and MEGs. IEEE Trans. Biomed. Eng., 1993, 40: 42–48.

Cuffin, B.N., Cohen, D., Yunokuchi, K., Maniewski, R., Purcell, C., Cosgrove, G.R., Ives, J., Kennedy, J. and Schomer, D. Tests of EEG localization accuracy using implanted sources in the human brain. Ann. Neurol., 1991, 29: 132–138.

Curio, G., Oppel, F. and Scherg, M. Peripheral origin of BAEP wave II in a case with unilateral pontine pathology: a comparison of intracranial and scalp records. Electroenceph. clin. Neurophysiol., 1987, 66: 29–33.

Dale, A.M. and Sereno, M.I. Improving localization of cortical activity by combining EEG and MEG with MRI cortical surface reconstruction: a linear approach. J. Cogn. Neurosci., 1993, 5: 162–176.

Ebersole, J.S. EEG dipole modeling in complex partial epilepsy. Brain Topogr., 1991, 4: 113–123.

Fender, D.H. Source localization of brain electrical activity. In: A.S. Gevins and A. Rémond (Eds.), Methods of Analysis of Brain Electrical and Magnetic Signals. Handbook of Electroencephalography and Clinical Neurophysiology, Vol. 1 (Revised Ser.). Elsevier, Amsterdam, 1987: 355–403.

Franssen, H., Stegeman, D.F., Moleman, J. and Schoobaar, R.P. Dipole modelling of median nerve SEPs in normal subjects and patients with small subcortical infarcts. Electroenceph. clin. Neurophysiol., 1992, 84: 401–417.

Hämäläinen, M.S. and Sarvas, J. Realistic conductivity geometry model of the human head for the interpretation of neuromagnetic data. IEEE Trans. Biomed. Eng., 1989, BME-36: 165–172.

Law, S.K., Nunez, P.L. and Wijesinghe, R.S. High-resolution EEG using spline generated surface Laplacians on spherical and ellipoidal surfaces. IEEE Trans. Biomed. Eng., 1993, 40: 145–153.

Lopes da Silva, F.H. and Spekreijse, H. Localization of brain sources of visually evoked responses: using single and multiple dipoles. An overview of different approaches. In: C.H.M. Brunia, G. Mulder and M.N. Verbaten (Eds.), Event-Related Brain Potential Research. Elsevier, Amsterdam, 1991: 38–46.

Meijs, J.W.H. and Peters, M.J. The EEG and MEG, using a model of eccentric spheres to describe the head. IEEE Trans. Biomed. Eng., 1987, BME-34: 913–920.

Meijs, J.W.H., Weier, O.W., Peters, M.J. and Van Oosterom, A. On the numerical accuracy of the boundary element method. IEEE Trans. Biomed. Eng., 1989, 36: 1038–1049.

Miltner, W. Ereigniskorrelierte Potentiale in der Schmerzmessung und Schmerzkontrolle. Habilitationsschrift. Medizinische Fakultät. Eberhard-Karls-Universität, Tübingen, 1989.

Mosher, J.C., Spencer, M.E., Leahy, R.M. and Lewis, P.S. Error bounds for EEG and MEG dipole source localization. Electroenceph. clin. Neurophysiol., 1993, 86: 303–321.

Nunez, P.L. Electric Fields of The Brain. Oxford University Press, New York, 1981.

Nunez, P.L. The brain's magnetic field: some effects of multiple sources on localization methods. Electroenceph. clin. Neurophysiol., 1986, 63: 75–82.

Nunez, P.L. Physical principles and neurophysiological mechanisms underlying event-related potentials. In: J.W. Rohrbaugh, R. Parasuraman and R. Johnson, Jr. (Eds.), Event-Related Brain Potentials. Basic Issues and Applications. Oxford University Press, New York, 1990: 19–36.

Nunez, P.L., Silberstein, R.B., Cadusch, P.J., Wijesinghe, R.S., Westdorp, A.F. and Srinivasan, R. A theoretical and experimental study of high resolution EEG based on surface Laplacians and cortical imaging. Electroenceph. clin. Neurophysiol., 1994, 90: 40–57.

O'Donnell, B.F., Cohen, R.A., Hokama, H., Cuffin, B.N., Lippa, C., Shenton, M.E. and Drachman, D.A. Electrical source analysis of auditory ERPs in medial temporal lobe amnestic syndrome. Electroenceph. clin. Neurophysiol., 1993, 87: 394–402.

Peters, M.J. and Wieringa, H.J. The influence of the volume conductor on electric source estimation. Brain Topogr., 1993, 5: 337–345.

Ponton, C.W., Don, M., Waring, M.D., Eggermont, J.J. and Masuda, A. Spatio-temporal source modeling of evoked potentials to acoustic and cochlear implant stimulation. Electroenceph. clin. Neurophysiol., 1993, 88: 478–493.

Praamstra, P. and Stegeman, D.F. On the possibility of independent activation of bilateral mismatch negativity (MMN) generators. Electroenceph. clin. Neurophysiol., 1992, 82: 67–80.

Roth, B.J., Balish, M., Gorbach, A. and Sato, S. How well does a three-sphere model predict positions of dipoles in a realistically shaped head? Electroenceph. clin. Neurophysiol., 1993, 87: 175–184.

Scherg, M. Spatio-temporal modelling of early auditory evoked potentials. Rev. Laryngol., 1984, 105: 163–170.

Scherg, M. Fundamentals of dipole source potential analysis. In: F. Grandori, G.L. Romani and M. Hoke (Eds.), Auditory Evoked Electric and Magnetic Fields. Topographic Mapping and Functional Localization. Advances in Audiology, Vol. 6. Karger, Basel, 1990: 40–69.

Scherg, M. and Von Cramon, D. A new interpretation of the generators of BAEP waves I–V: results of a spatio-temporal dipole model. Electroenceph. clin. Neurophysiol., 1985a, 62: 290–299.

Scherg, M. and Von Cramon, D. Two bilateral sources of the late AEP as identified by a spatio-temporal dipole model. Electroenceph. clin. Neurophysiol., 1985b, 62: 32–44.

Scherg, M. and Von Cramon, D. Evoked dipole source potentials of the human auditory cortex. Electroenceph. clin. Neurophysiol., 1986a, 65: 344–360.

Scherg, M. and Von Cramon, D. Psychoacoustic and electrophysiologic correlates of central hearing disorders in man. Eur. Arch. Psychiat. Neurol. Sci., 1986b, 236: 56–60.

Scherg, M. and Von Cramon, D. Dipole source potentials of the auditory cortex in normal subjects and patients with temporal lobe lesions. In: F. Grandori, M. Hoke and G.L. Romani (Eds.),

Auditory Evoked Magnetic Fields and Electric Potentials. Karger, Basel, 1989: 165–193.

Scherg, M., Vajsar, J. and Picton, T.W. A source analysis of the late human auditory evoked potentials. J. Cogn. Neurosci., 1989, 1: 336–355.

Simpson, G.V., Scherg, M., Ritter, W. and Vaughan, Jr., H.G. Localization and temporal activity functions of brain sources generating the human visual ERP. In: C.H.M. Brunia, A.W.K. Gaillard and A. Kok (Eds.), Psychophysiological Brain Research, Vol. 1. Tilburg University Press, Tilburg, 1990: 99–105.

Snyder, A.Z. Dipole source localization in the study of EP generators: a critique. Electroenceph. clin. Neurophysiol., 1991, 80: 321–325.

Speckmann, E., Caspers, H. and Elger, C.E. Neuronal mechanisms underlying the generation of field potentials. In: T. Elbert, B. Rockstroh, W. Lutzenberger and N. Birbaumer (Eds.), Self-Regulation of the Brain and Behavior. Springer, Berlin, 1984: 9–25.

Tarkka, I.M. and Treede, R.-D. Equivalent electrical source analysis of pain-related somatosensory evoked potentials elicited by a CO_2 laser. J. Clin. Neurophysiol., 1993, 10: 513–519.

Toro, C., Matsumoto, J., Deuschl, G., Roth, B.J. and Hallett, M. Source analysis of scalp-recorded movement-related electrical potentials. Electroenceph. clin. Neurophysiol., 1993, 86: 167–175.

Turetsky, B., Raz, J. and Fein, G. Representation of multi-channel evoked potential data using a dipole component model of intracranial generators: application to the auditory P300. Electroenceph. clin. Neurophysiol., 1990, 76: 540–556.

Zhang, Z. and Jewett, D.L. Insidious errors in dipole localization parameters at a single time-point due to model misspecification of number of shells. Electroenceph. clin. Neurophysiol., 1993, 88: 1–11.